

## Reaction Crystallization of Pharmaceutical Molecular Complexes

Naír Rodríguez-Hornedo,\* Sarah J. Nehm, Kurt F. Seefeldt,  
Yomaira Pagán-Torres, and Christopher J. Falkiewicz

Department of Pharmaceutical Sciences, University of Michigan,  
Ann Arbor, Michigan 48109-1065

Received November 7, 2005

**Abstract:** A mechanism for cocrystal synthesis is reported whereby nucleation and growth of cocrystals are directed by the effect of the cocrystal components on reducing the solubility of the molecular complex to be crystallized. The carbamazepine:nicotinamide cocrystal (CBZ:NCT) was chosen as a model system to study the reaction cocrystallization pathways and kinetics in aqueous and organic solvents. Fiber optic Raman spectroscopy and Raman microscopy were used for in situ monitoring of the cocrystallization in macroscopic and microscopic scales in solutions, suspensions, slurries, and wet solid phases of cocrystal components. This study demonstrates the advantages of reaction cocrystallization methods to develop rational approaches for high-throughput screening of cocrystals that can be transferable to control batch and continuous cocrystallization processes.

**Keywords:** Solution-mediated transformation; cocrystal; cocrystallization; solubility product; Raman spectroscopy

### Introduction

Understanding how molecules assemble by noncovalent bonds to form multiple component crystalline complexes or cocrystals is important for the design and discovery of pharmaceutical solids.<sup>1–6</sup> The improved physicochemical and pharmaceutical properties of cocrystals compared to the

single component crystal of a drug have been reported, such as dissolution rate, solubility, chemical stability, and moisture uptake.<sup>7–12</sup>

The key to designing these extended architectures lies in identifying intermolecular interactions that direct molecular assembly.<sup>13–17</sup> Hydrogen bonds, because of their strength and directionality, have been one of the most useful interactions

\* Corresponding author. Mailing address: College of Pharmacy, 428 Church St., Ann Arbor, MI 48109-1065. Phone: 734-763-0101. Fax: 734-615-6162. E-mail: nrh@umich.edu.

- (1) Etter, M. C.; Reutzel, S. M. Hydrogen Bond Directed Cocrystallization and Molecular Recognition Properties of Acyclic Imides. *J. Am. Chem. Soc.* **1991**, *113*, 2586–2598.
- (2) Etter, M. C. Hydrogen Bonds as Design Elements in Organic Chemistry. *J. Phys. Chem.* **1991**, *95*, 4601–4610.
- (3) Nangia, A.; Desiraju, G. R. Supramolecular Synthons and Pattern Recognition. *Top. Curr. Chem.* **1998**, *198*, 57–95.
- (4) Desiraju, G. R. Supramolecular Synthons in Crystal Engineering—A New Organic Synthesis. *Angew. Chem., Int. Ed. Engl.* **1995**, *34*, 2311–2327.
- (5) Nehm, S. J.; Rodríguez-Spong, B.; Rodríguez-Hornedo, N. Phase Solubility Diagrams of Cocrystals Are Explained by Solubility Product and Solution Complexation. *Cryst. Growth Des.* **2006**, *6*, 592–600.

- (6) Rodríguez-Spong, B.; Price, C. P.; Jayasankar, A.; Matzger, A. J.; Rodríguez-Hornedo, N. General Principles of Pharmaceutical Solid Polymorphism: A Supramolecular Perspective. *Adv. Drug Delivery Rev.* **2004**, *56*, 241–274.
- (7) Childs, S. L.; Chyall, L. J.; Dunlap, J. T.; Smolenskaya, V. N.; Stahly, B. C.; Stahly, G. P. Crystal Engineering Approach to Forming Cocrystals of Amine Hydrochlorides with Organic Acids. Molecular Complexes of Fluoxetine Hydrochloride with Benzoic, Succinic, and Fumaric Acids. *J. Am. Chem. Soc.* **2004**, *126*, 13335–13342.
- (8) Trask, A. V.; Motherwell, W. D. S.; Jones, W. Pharmaceutical Cocrystallization: Engineering a Remedy for Caffeine Hydration. *Cryst. Growth Des.* **2005**, *5*, 1013–1021.
- (9) Remenar, J. F.; Morissette, S. L.; Peterson, M. L.; Moulton, B.; MacPhee, J. M.; Guzman, H. R.; Almarsson, O. Crystal Engineering of Novel Cocrystals of a Triazole Drug with 1,4-Dicarboxylic Acids. *J. Am. Chem. Soc.* **2003**, *125*, 8456–8457.

in building these molecular networks. Many pharmaceutical molecules are known to form hydrogen bonded assemblies in solution and in the solid state and are therefore good reactants for supramolecular synthesis with other components. In fact, hydrogen bonds have been employed in the formation of crystalline supramolecular assemblies of binary and ternary composition where at least one of the components is a drug.<sup>7–9,18–23</sup>

Cocrystallization is an essential step in the successful synthesis of cocrystals. The most generally used solution-based method to synthesize these materials is slow evaporation from solutions of cocrystal components with stoichio-

metric composition.<sup>1,7,18,19,22–24</sup> Solvothermal methods are also reported in the literature, although less frequently.<sup>12,25</sup> These techniques, however, suffer from the risk of crystallizing the single component phases, thereby reducing the possibility of accessing the multicomponent crystalline phase. As a result of the empirical basis of the approaches used in search of cocrystals, a very large number of experimental conditions are often tested<sup>26</sup> and transferability to larger scale crystallization processes is limited.

In this brief article, we report a method for the rapid generation of cocrystals by reaction cocrystallization in microscopic and macroscopic scales under ambient conditions, where nucleation and cocrystallization are initiated by the effect of the cocrystal components on reducing the solubility of the molecular complex to be crystallized.<sup>5</sup> We also discuss the importance of the cocrystal solubility product in explaining the phase solubility diagram of cocrystals and in identifying conditions to prepare cocrystals in solutions, suspensions, slurries, or wet solid phases of cocrystal components. This method offers significant improvements over traditional cocrystallization methods in that it (1) is applicable to develop rational in situ techniques for high-throughput screening of cocrystals, (2) is transferable to larger scale cocrystallization processes, and (3) is more environmentally friendly.

The carbamazepine:nicotinamide cocrystal (CBZ:NCT) was chosen as a model system to study the reaction cocrystallization pathways and kinetics in aqueous and organic solvents. The crystal structure of CBZ:NCT has been reported<sup>18</sup> (refcode in the Cambridge Structural Database is UNEZES<sup>27</sup>) and is characterized by N–H···O=C hydrogen bonds between nicotinamide and carbamazepine molecules as shown in Figure 1. Nicotinamide in this structure hydrogen bonds with the carbamazepine carboxamide dimers forming a hydrogen bonded tape down the *a* crystallographic axis.

## Experimental Section

**Materials.** Anhydrous monoclinic carbamazepine (CBZ-(III), 5*H*-dibenz[*b,f*]azepine-5-carboxamide; Lot No. 093K1544 USP grade) was purchased from Sigma Chemical Company (St. Louis, MO), stored at 5 °C over anhydrous calcium

- (10) Zocharski, P.; Nehm, S.; Rodríguez-Spong, B.; Rodríguez-Hornedo, N. Can Solubility Products Explain Cocrystal Solubility and Predict Crystallization Conditions? *AAPS J.* **2004**, *6*, Abstract R6192.
- (11) Rodríguez-Spong, B.; Zocharski, P.; Billups, J.; McMahon, J.; Zaworotko, M. J.; Rodríguez-Hornedo, N. Enhancing the Pharmaceutical Behavior of Carbamazepine Through the Formation of Cocrystals. *AAPS J.* **2003**, *5*, Abstract M1298.
- (12) Rodríguez-Spong, B. Enhancing the Pharmaceutical Behavior of Poorly Soluble Drugs Through the Formation of Cocrystals and Mesophases. Ph.D. Thesis, University of Michigan, 2005.
- (13) Pedireddi, V. R.; Jones, W.; Chorlton, A. P.; Docherty, R. Creation of Crystalline Supramolecular Arrays: A Comparison of Cocrystal Formation from Solution and By Solid-state Grinding. *Chem. Commun.* **1996**, 987–988.
- (14) Etter, M. C. Encoding and Decoding Hydrogen-Bond Patterns of Organic Compounds. *Acc. Chem. Res.* **1990**, *23*, 120–126.
- (15) Desiraju, G. R. Hydrogen Bridges in Crystal Engineering: Interactions without Borders. *Acc. Chem. Res.* **2002**, *35*, 565–573.
- (16) Desiraju, G. R. Designer Crystals: Intermolecular Interactions, Network Structures and Supramolecular Synthons. *Chem. Commun.* **1997**, 1475–1482.
- (17) Leiserowitz, L.; Schmidt, G. M. J. Molecular Packing Modes. Part III. Primary Amides. *J. Chem. Soc. A* **1969**, 2372–2382.
- (18) Fleischman, S. G.; Kuduva, S. S.; McMahon, J. A.; Moulton, B.; Walsh, R. D. B.; Rodríguez-Hornedo, N.; Zaworotko, M. J. Crystal Engineering of the Composition of Pharmaceutical Phases: Multiple-Component Crystalline Solids Involving Carbamazepine. *Cryst. Growth Des.* **2003**, *3*, 909–919.
- (19) Walsh, R. D. B.; Bradner, M. W.; Fleischman, S.; Morales, L. A.; Moulton, B.; Rodríguez-Hornedo, N.; Zaworotko, M. J. Crystal Engineering of the Composition of Pharmaceutical Phases. *Chem. Commun.* **2003**, 186–187.
- (20) Vishweshwar, P.; McMahon, J.; Peterson, M. L.; Hickey, M. B.; Shattock, T. R.; Zaworotko, M. J. Crystal Engineering of Pharmaceutical Co-crystals from Polymorphic Active Pharmaceutical Ingredients. *Chem. Commun.* **2005**, 4601–4603.
- (21) Madarasz, J.; Bombicz, P.; Jarmi, K.; Ban, M.; Pokol, G.; Gal, S. Thermal, FTIR and XRD Study on Some 1:1 Molecular Compounds of Theophylline. *J. Therm. Anal. Calorim.* **2002**, *69*, 281–290.
- (22) Caira, M. R. Molecular Complexes of Sulfonamides. Part 1. 1:1 Complexes Between Sulfadimidine [4-amino-N-(4,6-dimethyl-2-pyrimidinyl)benzenesulfonamide] and 2- and 4-aminobenzoic acids. *J. Crystallogr. Spectrosc. Res.* **1991**, *21*, 641–648.
- (23) Caira, M. R. Molecular Complexes of Sulfonamides. 2. 1:1 Complexes Between Drug Molecules: Sulfadimidine-acetylsalicylic acid and Sulfadimidine-4-aminosalicylic acid. *J. Crystallogr. Spectrosc. Res.* **1992**, *22*, 193–200.
- (24) Ghosh, M.; Basak, A. K.; Mazumdar, S. K. Structure and Conformation of the 1:1 Molecular Complex of Sulfaproxyline-Caffeine. *Acta Crystallogr.* **1991**, *C47*, 577–580.
- (25) Bettinetti, G.; Caira, M. R.; Callegari, A.; Merli, M.; Sorrenti, M.; Tadini, C. Structure and Solid-State Chemistry of Anhydrous and Hydrated Crystal Forms of the Trimethoprim-Sulfamethoxypyridazine 1:1 Molecular Complex. *J. Pharm. Sci.* **2000**, *89*, 478–489.
- (26) Morissette, S. L.; Almarsson, O.; Peterson, M. L.; Remenar, J. F.; Read, M. J.; Lemmo, A. V.; Ellis, S.; Cima, M. J.; Gardner, C. R. High-throughput Crystallization: Polymorphs, Salts, Cocrystals and Solvates of Pharmaceutical Solids. *Adv. Drug Delivery Rev.* **2004**, *56*, 275–300.
- (27) Allen, F. H. The Cambridge Structural Database: A Quarter of a Million Crystal Structures and Rising. *Acta Crystallogr.* **2002**, *B58*, 380–388.

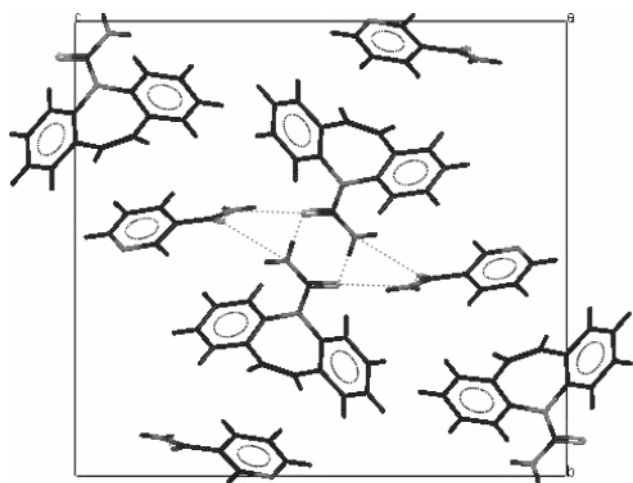


**Figure 1.** Crystal structure of CBZ:NCT viewed down the *a* crystallographic axis showing the molecular assembly.

sulfate, and used as received. Nicotinamide (NCT(I), pyridine-3-carboxylic acid amide; Lot No. 122K0077) was purchased from Sigma Chemical Company (St. Louis, MO) and used as received. Solid state forms were identified by X-ray powder diffraction.

Ethyl acetate and 2-propanol were of HPLC grade and were purchased from Fisher Scientific (Fair Lawn, NJ). Anhydrous ethanol (200 proof) was USP grade and was purchased from Pharmco (Brookfield, CT).

**Solubility of CBZ:NCT.** The equilibrium solubility of CBZ:NCT cocrystal was determined from undersaturation by adding excess cocrystal solid phase to pure ethanol and ethanol solutions of NCT ranging between 0.05 and 0.20 M. The suspensions were stirred with magnetic stirrers in 20 mL glass vials at constant temperature ( $25 \pm 0.5$  °C) maintained with a circulating temperature bath (Neslab RTE-110, Portsmouth, NH). Samples were drawn at 48 h using a  $0.45 \mu\text{m}$  PTFE filter (Fisherbrand, Pittsburgh, PA) and were diluted with ethanol. CBZ concentrations were calculated by measuring the absorbance of CBZ ( $\lambda_{\text{max}} = 284$  nm) by UV/vis spectroscopy (Beckman DU-650, Fullerton, CA). The CBZ concentration corresponds to the CBZ:NCT solubility based on the 1:1 molar ratio cocrystal.

**Raman Spectroscopy.** Raman spectra were collected with a Kaiser Optical Systems, Inc. (Ann Arbor, MI), RXN1 Raman spectrometer equipped with a 785 nm laser and a  $1/4$  in. fiber optic immersion probe. Crystallization and dissolution were monitored in situ in macrophases with the probe and in microphases using a Leica DMLP (Wetzlar, Germany) Raman microscope. Acquisition conditions were optimized so that the spectra collected had maximum intensity above  $8 \times 10^6$  counts. The spectra collected had a spectral resolution of  $4 \text{ cm}^{-1}$  and were collected between 100 and  $3200 \text{ cm}^{-1}$ . Solid phases were characterized by Raman spectroscopy (Supporting Information Figure 1).

**Polarized Optical Microscopy.** Crystallization in microphases was visually monitored with a Leica DMPL polarizing optical microscope (Wetzlar, Germany). Images were col-

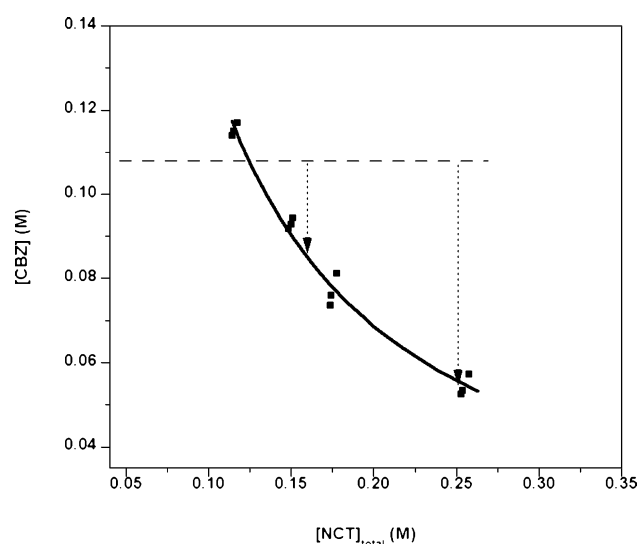


**Figure 2.** Phase solubility diagram of carbamazepine:nicotinamide (1:1) cocrystal as a function of cocrystal component concentration in ethanol at 25 °C. The solid line represents the predicted solubility according to eq 3 with a solubility product  $K_{\text{sp}} = 0.0129 \text{ M}^2$ . The dashed line represents the solubility of CBZ(III) in ethanol, 0.108 M. The dotted arrows represent the cocrystallization conditions studied.

lected with a Spot Insight FireWire 4 Megasample Color Mosaic camera controlled with Spot software (Diagnostics Inc, Sterling Heights, MI). Solid phases crystallized were identified by Raman microscopy.

**X-ray Powder Diffraction (XRPD).** X-ray powder diffraction patterns of solid phases were recorded with a Rigaku MiniFlex X-ray diffractometer (Danvers, MA) using Cu  $K\alpha$  radiation ( $\lambda = 1.54 \text{ \AA}$ ), a tube voltage of 30 kV, and a tube current of 15 mA. The intensities were measured at  $2\theta$  values from  $2^\circ$  to  $50^\circ$  at a continuous scan rate of  $2.5^\circ/\text{min}$ . Solid phases at equilibrium during solubility experiments were analyzed by X-ray powder diffraction, and results were compared to the diffraction patterns calculated from the crystal structure reported in the Cambridge Structural Database<sup>27</sup>(Supporting Information Figures 2–5).

**Infrared (IR) Spectroscopy.** FTIR spectra of solid phases were collected on a Bruker Vertex 70 FT-IR (Billerica, MA) unit equipped with a DTGS detector. Samples were placed on a zinc selenide (ZnSe) attenuated total reflectance (ATR) crystal accessory, and 64 scans were collected for each sample at a resolution of  $4 \text{ cm}^{-1}$  over a wavenumber region of  $4000\text{--}600 \text{ cm}^{-1}$ .

## Results and Discussion

The phase solubility diagram for the carbamazepine:nicotinamide cocrystal (CBZ:NCT) as a function of the ligand or cocrystal component concentration (NCT) in ethanol solutions is shown in Figure 2. This solubility study reveals that addition of cocrystal component to solutions in excess of the stoichiometric composition reduces the cocrystal solubility and is explained by considering the equi-

librium reaction for a binary cocrystal A:B dissociating in solution to A and B according to



where A represents API or CBZ and B represents ligand or cocrystal component or NCT. Subscripts refer to the stoichiometric number of molecules of A or B in the cocrystal. The equilibrium constant for this reaction is given by

$$K_{\text{eq}} = \frac{a_A^a a_B^b}{a_{A:B}} \quad (2)$$

and is proportional to the thermodynamic activity product of the cocrystal components. If the activity of the solid is equal to 1 or is constant, the cocrystal solubility can be described by a solubility product

$$K_{\text{sp}} = a_A^a a_B^b \approx [A]^a [B]^b \quad (3)$$

where [A] and [B] are the molar concentrations of each cocrystal component at equilibrium, as long as the activity coefficients are unity. This equation predicts that addition of either cocrystal component in excess of its stoichiometric composition will decrease the cocrystal solubility, in agreement with the observed trend in Figure 2. Mathematical models that consider solution complexation equilibria and solubility of solid state complex or cocrystal have been derived and are presented elsewhere.<sup>5</sup> It is important to note that the solubility predicted by the solubility product alone is smaller than the solubility in the presence of solution complexes, as shown by the equations that follow.

In the case of 1:1 solution complexes the cocrystal solubility is given by

$$[A]_T = \frac{K_{\text{sp}}}{[B]_T - K_{11}K_{\text{sp}}} + K_{11}K_{\text{sp}} \quad (4)$$

If  $K_{11}K_{\text{sp}} \ll [B]_T$ , then

$$[A]_T = \frac{K_{\text{sp}}}{[B]_T} + K_{11}K_{\text{sp}} \quad (5)$$

This equation predicts that cocrystal solubility is higher than the value calculated in the absence of solution complexation by a constant value, the product of the complexation constant and the solubility product,  $K_{11}K_{\text{sp}}$ . In the absence of solution complexation,  $K_{11} = 0$ , the cocrystal solubility is predicted by the solubility product alone. In the case of 1:1 and 1:2 solution complexes the cocrystal solubility initially decreases, passes through a minimum at  $[B] = [1/(K_{11}K_{12})]^{1/2}$ , and then increases.

The solubility product of CBZ:NCT cocrystal in ethanol solutions was determined to be  $K_{\text{sp}} = 0.0129 \text{ M}^2$  by plotting  $[A]_T$  versus  $1/[B]_T$  according to eq 5, using the measured cocrystal solubilities shown in Figure 2. Linear regression results showed that the intercept is not significantly different from zero and suggest that solution complexation is negli-

gible in this solvent.<sup>5</sup> The cocrystal solubility predicted by the solubility product alone is shown in Figure 2 and is in excellent agreement with the experimentally measured solubility. These results demonstrate that there is a common cocrystal component effect on cocrystal solubility, similar to that of the common ion effect in the case of sparingly soluble salts.<sup>28–31</sup>

On the basis of this solubility behavior, we developed reaction cocrystallization methods under ambient conditions, where nucleation and crystallization of the molecular complex are directed by decreasing the solubility of the molecular complex to be crystallized. Supersaturation is the driving force for crystallization and can be generated by adding excess cocrystal component to a solution so that non-stoichiometric concentrations are achieved. As nicotinamide is added to solutions of ethanol, the solubility of CBZ:NCT cocrystal decreases below the solubility of the pure anhydrous CBZ(III) as shown in Figure 2. In pure ethanol the solubilities of CBZ:NCT cocrystal and CBZ(III) single component crystal are similar,  $0.116 \pm 0.003 \text{ M}$  and  $0.1080 \pm 0.0001 \text{ M}$ . However, the solubility ratio (cocrystal/CBZ(III)) is decreased from 1.07 in pure ethanol to 0.48 in 0.25 M NCT.

With the purpose of investigating the rates of cocrystallization under the conditions described by the solubility product behavior, we studied the cocrystallization of CBZ:NCT in organic solutions (ethanol, 2-propanol, or ethyl acetate) and in aqueous solutions in micro- and macrophases. Reaction cocrystallizations were studied in suspensions of reactant or reactants and in solutions of reactants as described below.

The cocrystallization of CBZ:NCT by dissolving anhydrous CBZ(III) (385 mg) in ethanol solutions of NCT 0.16 M (10 mL) was monitored by Raman spectroscopy as shown in Figure 3. This amount of CBZ is higher than the solubility of CBZ(III) in ethanol by 50.8%. The shift in the Raman peak with respect to time, from  $722$  to  $718 \text{ cm}^{-1}$ , indicates that pure CBZ(III) transformed to CBZ:NCT cocrystal within 3 h. These results suggest a solution-mediated transformation where dissolution of pure CBZ creates supersaturated conditions with respect to cocrystal and leads to cocrystallization of CBZ:NCT. When one of the reactants is in the solid state and in an amount greater than its solubility value, it is consumed by the cocrystallization reaction, as shown in this case, and the final product is the cocrystalline phase.

Increasing the NCT concentration in the experiment above to 0.25 M resulted in faster conversion of pure anhydrous CBZ(III) to cocrystal, within 2–3 min. This time was shorter

- (28) Rodríguez-Clemente, R. Complexing and Growth Units in Crystal Growth from Solutions of Electrolytes. *J. Cryst. Growth* **1989**, 98, 617–629.
- (29) Nielsen, A. E.; Toft, J. M. Electrolyte Crystal Growth Kinetics. *J. Cryst. Growth* **1984**, 67, 278–288.
- (30) Khankari, R. K.; Grant, D. J. W. Pharmaceutical Hydrates. *Thermochim. Acta* **1995**, 248, 61–79.
- (31) Tomazic, B.; Nancollas, G. H. The Kinetics of Dissolution of Calcium Oxalate Hydrates. *J. Cryst. Growth* **1979**, 46, 355–361.

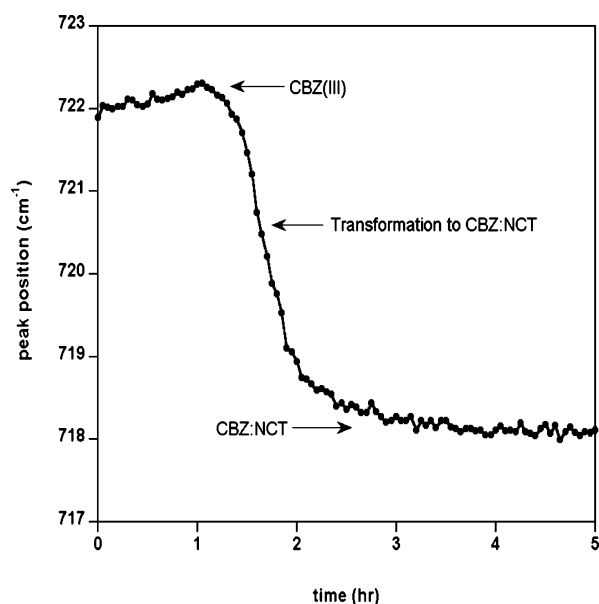


**Figure 3.** Raman peak position with respect to time showing the slurry conversion or transformation of solid phase CBZ(III) to cocrystal CBZ:NCT at 25 °C after adding 0.16 M solution of nicotinamide in ethanol to CBZ(III).

than that required to collect the Raman spectra, and the time course for this transformation is not shown. Increasing NCT concentration in the dissolution/cocrystallization medium increased the initial supersaturation with respect to cocrystal and significantly increased the cocrystallization rate as shown by the shorter times for transformation to cocrystal from 3 h to 3 min. The supersaturation,  $\sigma$ , for a cocrystal is derived from the difference in chemical potential between the supersaturated solution state and the saturated solution state<sup>12</sup> and is given by

$$\sigma = \left( \frac{\prod c_i^{\nu_i}}{K_{sp}} \right)^{1/\nu} \quad (6)$$

where  $\prod c_i^{\nu_i}$  is the product of the concentration of cocrystal components in the supersaturated solution when the activity coefficients are unity,  $\nu$  is the stoichiometric coefficient in the chemical equation or stoichiometric number of cocrystal components,  $i$ , in the cocrystal chemical formula  $\nu = \sum \nu_i$ , and  $K_{sp}$  is the solubility product. The supersaturation with respect to a (1:1) cocrystal, such as CBZ:NCT, is expressed by

$$\sigma = \left( \frac{[\text{CBZ}][\text{NCT}]}{K_{sp}} \right)^{1/2} \quad (7)$$

Equation 7 shows that supersaturation and crystallization rate can be increased by increasing the concentration of individual components.

A priori knowledge of the solubility of cocrystal in pure solvent is useful to predict the cocrystal phase solubility diagram as a function of ligand concentration and to determine conditions under which cocrystals dissolve or precipitate.<sup>5</sup> Figure 4 shows that CBZ:NCT cocrystal can

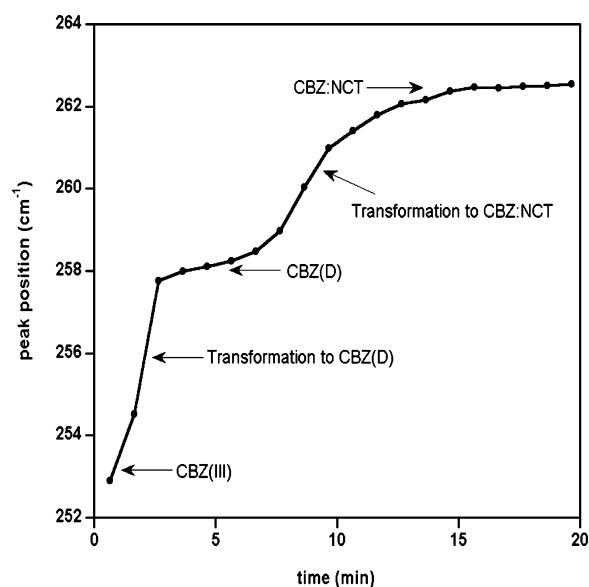


**Figure 4.** Raman peak position with respect to time showing the slurry conversion or solution-mediated transformation of anhydrous CBZ(III) to cocrystal CBZ:NCT in water saturated with nicotinamide at 23 °C according to the following pathway: CBZ(III) → CBZ(D) → CBZ:NCT.

be prepared in water by suspending anhydrous CBZ(III) in saturated solutions of nicotinamide at room temperature. It is interesting to note that anhydrous CBZ(III) transforms to dihydrate CBZ, CBZ(D), and then cocrystal in this aqueous suspension, and suggests that the order of the solubility is CBZ(III) > CBZ(D) > CBZ:NCT. This is an important finding since in pure water at room temperature the solubility of CBZ:NCT is greater than that of CBZ(D), and cocrystal transforms to CBZ(D).<sup>11,12</sup> The reason for this reversal in transformations is the reduced solubility of cocrystal by addition of cocrystal component, nicotinamide, to solution in excess of the cocrystal stoichiometry.

CBZ:NCT cocrystal was also prepared in situ in covered depression slides on the polarizing optical light and Raman microscopes by addition of a small drop of solvent (ethanol, ethyl acetate, or 2-propanol) to the solid reactants, CBZ(III) and NCT(I). Photographs from the ethyl acetate experiment obtained through the polarized light microscope are shown in Figure 5. These images show cocrystal formation in less than 3 min after ethyl acetate addition. The solid phase of the product was confirmed to be CBZ:NCT cocrystal by Raman microscopy. Similar behavior was observed by using microphases of ethanol or 2-propanol. In this case the cocrystallization reaction proceeds by a pathway similar to those of macrophase suspensions described above. In microphases the solvent added must allow for dissolution of both reactants so that nonstoichiometric concentrations generate the supersaturation required for crystallization of the complex, as shown in Figure 6. For instance, Figure 5b shows unreacted CBZ(III) in an isolated drop where cocrystallization had not occurred in the time course of the experiment due to lower concentrations of NCT than in other regions of the sample.

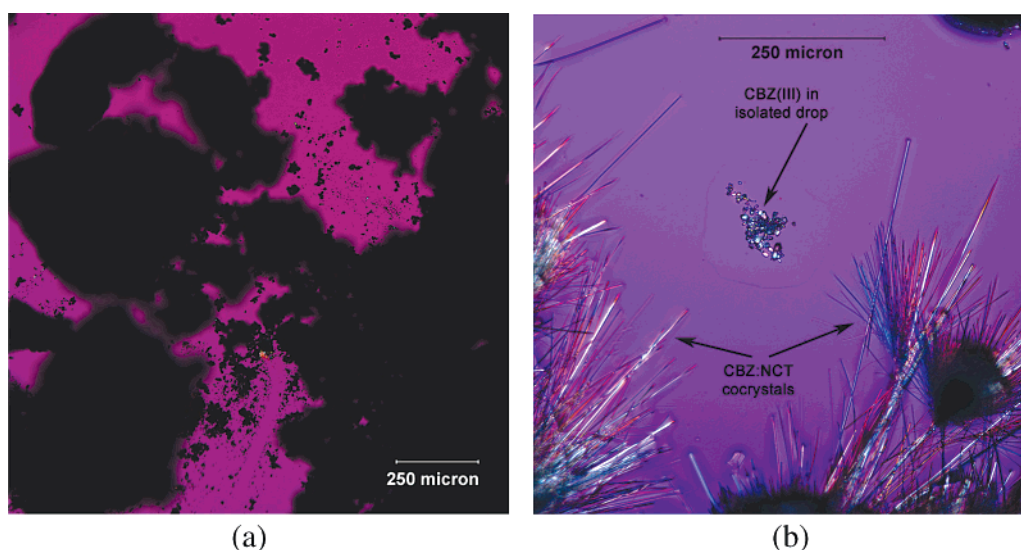


**Figure 5.** Photomicrographs of CBZ(III) and NCT(I) (a) before addition of ethyl acetate and (b) 3 min after addition of a small drop of ethyl acetate. Needles were confirmed to be cocrystal CBZ:NCT by Raman microscopy.

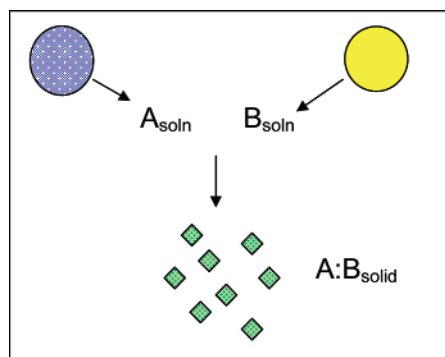


**Figure 6.** Cocrystallization of molecular complex A:B from the supersaturation generated by the dissolution of solid reactants, A and B, in a microphase of solvent.

Precipitation or reaction cocrystallization was also achieved by mixing solutions of reactants or cocrystal components in nonstoichiometric concentrations according to the solubility product behavior. CBZ:NCT cocrystal was prepared by mixing solutions of CBZ and NCT in the same solvent. Solvents studied included ethanol, 2-propanol, and ethyl acetate. Cocrystals were observed within 10–25 min ( $n = 4$ ) after initial gentle mixing of an ethanol solution of NCT (2.25 mL of 0.8 M) and an ethanol solution of CBZ (3.75 mL of 0.1 M). Similar behavior was observed in 2-propanol and ethyl acetate.

Studies with other cocrystalline systems are underway, in an effort to confirm the general applicability of the phase diagrams, mechanisms, and cocrystallization methods presented here. Transformation to cocrystal from single-component solid reactants has also been observed for sulfadimidine:anthranilic acid and sulfadimidine:salicylic acid from acetonitrile, ethanol, and water and carbamazepine:saccharin from water and 0.1 N HCl (Supporting Information Figures 6–9).

## Conclusions

The results presented here demonstrate that reaction cocrystallization allows for the effective and rapid formation of cocrystals under ambient conditions, in micro- and macrophases of aqueous and organic solvents or solutions. This research also identifies the mechanism for cocrystal formation from solutions or solid–liquid systems (slurries or wet solid phases), where cocrystallization is initiated by the effect of nonstoichiometric concentrations of cocrystal components on reducing the solubility of the molecular complex to be crystallized. These findings provide a powerful approach to develop rational screening methods for cocrystal discovery, and in situ cocrystallization techniques, as well as to develop batch and continuous cocrystallization processes. The solubility product behavior indicates that a wider range of solvents can be used for cocrystallization, with the advantage over traditional methods that cocrystallization is no longer limited by the different solubilities of the components, and will lead to environmentally friendly methods for cocrystal synthesis.

**Acknowledgment.** We gratefully acknowledge funding from GM07767 National Institute of General Medical Sciences (NIGMS) for S.J.N and from the College of Pharmacy, University of Michigan. The contents of this publication are solely the responsibility of the authors and do not necessarily represent the official views of funding sources.

**Supporting Information Available:** Spectroscopic and X-ray powder diffraction diagrams of reactants (cocrystal components) and cocrystals. This material is available free of charge via the Internet at <http://pubs.acs.org>.

MP050099M